

## Phonon spectrum of YBCO obtained by specific heat inversion method for real data

This article has been downloaded from IOPscience. Please scroll down to see the full text article.

2003 J. Phys.: Condens. Matter 15 225

(<http://iopscience.iop.org/0953-8984/15/2/322>)

View [the table of contents for this issue](#), or go to the [journal homepage](#) for more

Download details:

IP Address: 171.66.16.119

The article was downloaded on 19/05/2010 at 06:28

Please note that [terms and conditions apply](#).

# Phonon spectrum of YBCO obtained by specific heat inversion method for real data

Tao Wen<sup>1</sup>, GuiCun Ma<sup>1</sup>, XianXi Dai<sup>1,4</sup>, JiXin Dai<sup>2</sup> and William E Evenson<sup>3</sup>

<sup>1</sup> Group of Quantum Statistics & Method of Theoretical Physics and Surface Physics Laboratory, Department of Physics, Fudan University, Shanghai 200433, People's Republic of China

<sup>2</sup> Department of Chemistry, New York University, NY 10003, USA

<sup>3</sup> Department of Physics and Astronomy, Brigham Young University, Provo, UT 84602, USA

E-mail: xxdai@fudan.ac.cn

Received 25 September 2002

Published 20 December 2002

Online at [stacks.iop.org/JPhysCM/15/225](http://stacks.iop.org/JPhysCM/15/225)

## Abstract

In this paper, the phonon spectrum of YBCO is obtained from experimental specific heat data by an exact inversion formula with a parameter for eliminating divergences. The results can be compared to those of neutron inelastic scattering, which can only be carried out in a few laboratories. Some key points of specific heat-phonon spectrum inversion (SPI) theory and a method of asymptotic behaviour control are discussed. An improved unique existence theorem is presented, and a universal function set for numerical calculation of SPI is calculated with high accuracy, which makes the inversion method applicable and convenient in practice. This is the first time specific heat-phonon SPI has been realized for a concrete system.

## 1. Introduction

The specific heat-phonon spectrum inversion (SPI) has attracted theoretical and application interest for many years. But up to now, no one has been successful in obtaining the phonon spectrum directly from specific heat data. In this paper, we report the inversion of specific heat data for YBCO<sub>6,92</sub> to obtain the phonon spectrum, the first time such an inversion has been carried out for a concrete system. We also report the development of a universal function set (UFS) for this calculation. In the present paper the inversion procedure is discussed in detail.

We begin with the renormalized effective Hamiltonian of the lattice vibration system:

$$\hat{H} = \sum_{\vec{q}} \hbar \omega_{\vec{q}} \hat{b}_{\vec{q}}^{\dagger} \hat{b}_{\vec{q}}. \quad (1)$$

<sup>4</sup> Author to whom any correspondence should be addressed.

From this Hamiltonian, the lattice specific heat takes the form

$$C_V(T) = k_B \int_0^\infty \left( \frac{\hbar\omega}{k_B T} \right)^2 \frac{\exp(\hbar\omega/k_B T)}{[\exp(\hbar\omega/k_B T) - 1]^2} g(\omega) d\omega, \quad (2)$$

where  $g(\omega)$ ,  $T$ ,  $k_B$  and  $\hbar$  are the phonon density of states or phonon spectrum, temperature, Boltzmann constant and Planck constant, respectively.

According to equation (2), if  $g(\omega)$  is given, the specific heat can be obtained by integration. Its inverse problem is to extract the phonon spectrum from the specific heat by solving an integral equation.

Since 1989, two exact solution formulae for specific heat-phonon SPI have been published: Dai's formula with a parameter  $s$  cancelling the divergence [1, 2] and Chen's formula with a modified Möbius inversion formula [3, 4]. Both are closely related to the fundamentals of number theory, such as the properties of the Riemann zeta function in the complex plane and the Möbius inversion formula. Prior to our recent work, to the best of our knowledge no one has been able to realize SPI for a real, physical system. This paper gives the details of the theory that was developed for that purpose.

Because Dai's formula [2] yields both the exact Debye and Einstein spectra rigorously in closed form from their respective specific heats, we begin our study with that work. The following exact solution formula was derived:

$$g(\omega) = \frac{1}{\omega} \int_{-\infty}^{+\infty} \left( \frac{\omega}{T_0} \right)^{ik+s} \frac{\tilde{Q}_0(k) dk}{(ik+s+1)\Gamma(ik+s+1)\zeta(ik+s+1)}, \quad (3)$$

where  $\tilde{Q}_0(k)$  is the Fourier transform of  $Q_0(x)$ , given by

$$Q_0(x) = C_V(T_0 e^x) e^{-sx}. \quad (4)$$

One can therefore use equation (3) with known  $C_V$  to obtain the phonon spectrum directly. This solution uses the Fourier transform method [1, 2] to give an exact solution formula with parameter  $s$  cancelling divergences. A unique existence theorem for the solution in this form was also found.

As pointed out in [1, 2], if we let  $s = 0$ , the Riemann zeta function  $\zeta(ik+1)$  in the denominator lies in the Riemann strip. The Riemann hypothesis is an unsolved problem of more than 100 years standing. Although Hadamard [5] proved that for  $z = ik$  and  $1+ik$ ,  $\zeta(z)$  has no zeros, the parameter  $s$  is still needed to cancel the divergence in the Fourier transforms, because in general,

$$\lim_{T \rightarrow \infty} C_V(T) = \text{constant}. \quad (5)$$

This means that the Fourier transform of  $Z(x) \equiv C_V(T_0 e^x)$  does not exist in the class of classical functions. Even in the class of generalized functions, this Fourier transform is numerically unstable. We manage this problem by letting  $Q_0(x) = Z(x) e^{-sx}$ . If we take  $C_V \sim AT^{s_1}$  as  $T \rightarrow \infty$ , then  $s_1 = 0$ , giving one bound on the  $s$  that is needed to get a well behaved  $\tilde{Q}_0(k)$ . In the other limit,

$$\lim_{T \rightarrow 0} C_V(T) \sim AT^{s_2}, \quad (6)$$

and in many cases  $s_2 \approx D$ , the dimensionality of the lattice vibration system. Again, the Fourier transform can be divergent or ill behaved. This time the problem will occur if  $s$  is larger than  $s_2$ . So we choose

$$0 = s_1 < s < s_2 \approx D. \quad (7)$$

It is proven in [1, 2] that as long as we choose  $0 < s < D$ , a unique existence theorem is satisfied. This conclusion is independent of the Riemann hypothesis and Hadamard's proof. It

can also be proven that the exact solutions are  $s$  independent when  $0 < s < D$ . The solutions of Montroll [6], Lifshitz [7], and Chambers [8] all fall into the special case  $s = 1$ .

Another interesting inversion method, based on the modified Möbius inversion formula, was developed in the work of Chen [3]. We compare our method with Chen's method later in this paper.

In section 2, we discuss the challenges presented by the inversion problem and how this work deals with them. In section 3, the key points of the universal function method (UFM) are introduced. In section 4, results obtained by UFM are shown and analysed.

## 2. Problems and challenges

Even if one has an exact solution to a problem in principle, many new difficulties always come up when applying the new theoretical method to concrete systems. The purpose of this paper is to obtain the phonon spectrum from experimental specific heat data by using our exact solution formula described in the previous section. We investigate the YBCO specific heat and phonon spectrum because of the excellent experimental data available for the specific heat [9, 10] and for the phonon spectrum [11] as well as high interest in high  $T_c$  superconductivity (HTS). The phonon spectrum is intimately connected to conventional superconductivity and may be important in the mechanism of HTS.

The problems arising in developing a practical SPI procedure include the following:

- (1) experimental errors and limited range of data;
- (2) the difference between  $C_p$  (measured) and  $C_V$  (used in the theory);
- (3) separation of the lattice specific heat from the total specific heat;
- (4) the ill-posedness of the inversion problem;
- (5) asymptotic behaviour control (ABC);
- (6) finding a suitable basis of functions to expand in the function space.

### 2.1. Choice of data, $C_p$ versus $C_V$ , and separation of the lattice specific heat

It is essential that the specific heat data have suitable accuracy (for example, relative errors of  $\leq 10^{-4}$ ) and that they cover a sufficiently large temperature region (so there are data, at minimum, from low temperatures where  $C_V \sim AT^{3/2}$  to high temperatures where  $C_V$  approaches a constant). We will see later that this condition on the range of the data is essential for controlling asymptotic behaviour. Furthermore, in the case of YBCO, the oxygen concentration must be well controlled through the whole temperature region, so that the data correspond to a consistent material.

When selecting the experimental data for this study, we found that most existing experimental data could not satisfy the above conditions. We eventually found the experimental work of Bessergenev *et al* [9] on YBCO<sub>6.92</sub> to be suitable for inversion. The oxygen concentration is well controlled in a wide temperature region, and the data were taken with high accuracy. The experimental temperature region covers the interval mentioned above.

Experimental data are taken at constant pressure. But in the inversion problem we need the specific heat at constant volume. The difference between  $C_p$  and  $C_V$  is very small for solids [12], so we have neglected this difference in the present work.

Equation (1) applies to the lattice specific heat, but the measured data include contributions from both electrons and phonons. Above  $T_c$ , the electronic specific heat  $C_{el}$  is linear:  $C_{el} = \gamma T$ , where  $\gamma$  is the Sommerfeld constant. Below  $T_c$ , the electronic specific heat is determined by the microscopic mechanism of HTS. But this mechanism is not yet known.

As a first try and a suitable approximation, BCS theory has been adopted to find  $C_{el}$  in the superconducting phase. This theory can at least approximately describe the specific heat discontinuity at  $T_c$ . Then in  $\text{J mol}^{-1} \text{K}^{-1}$

$$C_{el} = \begin{cases} 3.15t^{-3/2}e^{-1.764/t} & t < 0.17 \\ 8.5e^{-1.44/t} & 0.17 \leq t < 0.5 \\ 2.43 + 3.77(t - 1) & 0.5 \leq t < 1.0, \end{cases}$$

where  $t = T/T_c$ . This approximation will be discussed further in the conclusion to this paper.

The experimental data are, of course, discrete. We obtained the following expression for the lattice specific heat of  $\text{YBCO}_{6.92}$  by fitting the data found in [9]:

$$C_V(T) = \begin{cases} a_1 T^{a_2} \exp\left(-\frac{a_3}{T + a_4}\right) & T < 16 \text{ K} \\ b_1 T \exp\left(-\frac{b_2}{T}\right) & 16 \text{ K} \leq T < 45 \text{ K} \\ \frac{c_1 - c_2}{\exp\left(\frac{T - X_0}{x_d}\right) + 1} + c_2 & T \geq 45 \text{ K}, \end{cases} \quad (8)$$

where  $a_1 = 0.17 \text{ J mol}^{-1} \text{K}^{-3}$ ,  $a_2 = 2.0$ ,  $a_3 = 117.7 \text{ K}$ ,  $a_4 = 20.0 \text{ K}$ ,  $b_1 = 2.8 \text{ J mol}^{-1} \text{K}^{-2}$ ,  $b_2 = 50.7 \text{ K}$ ,  $c_1 = -1109.4 \text{ J mol}^{-1} \text{K}^{-1}$ ,  $c_2 = 301.6 \text{ J mol}^{-1} \text{K}^{-1}$ ,  $X_0 = -110.3 \text{ K}$  and  $x_d = 105.0 \text{ K}$ . This expression was constrained to fit the data within experimental accuracy and to have asymptotic behaviour  $AT^{s_2}$  at low temperatures and approach a constant at high temperatures. The data were fitted to this expression by least squares. It can be seen from the above fitted expression that the main contribution to the lattice specific heat is of two-dimensional character and is controlled by the third law and the Dulong–Petit law.

In obtaining a continuous fitted form for  $C_V(T)$ , the third law and the Dulong–Petit law are used to control the asymptotic behaviours. The fitted expression is also useful for carrying out the inversion. In this way, data incompleteness has been overcome simultaneously and naturally by using the physics of this system to control asymptotic behaviour. This fitted curve provides the starting point for the numerical calculations.

In the above fitting procedure, any extra error that is introduced is concentrated at the following points:

- (1) the separation of the electronic specific heat,
- (2) the extension of the temperature region beyond the experimental data and
- (3) the accuracy of the fitting function.

## 2.2. Instability of solutions—inversion as an ill posed problem

It would appear that one should be able to calculate the phonon spectrum using equation (3) easily and uniquely in view of the unique existence theorem [2]. But for a real system, there are many fundamental and challenging problems still to be confronted. We now address the problem of instability arising from the fact that inversion is an ill posed problem.

A famous example of an ill posed problem in mathematics is that of Fredholm integral equations of the first kind. Even if the solution exists uniquely, a small deviation in the input may cause a large variation in the solution. Ill posed problems present difficulties in many inversion problems. Many attempts have been made to overcome this instability, including the maximum entropy method, the Tikhonov regulation method etc. But with respect to SPI, all such studies have so far dealt with artificial ‘specific heats’, and no one has previously realized phonon SPI from the specific heat using real data.

The resolution of instability problems lies in the function class that is defined and in applying physical constraints. This point can be seen clearly in studies of singular states in quantum mechanics [13], i.e. why some singular states are physical and others are not. The resolution of this problem lies in the natural laws that physical states must obey, e.g. orthogonality criteria. Such criteria select the physical states from the function class.

So in the inversion problem, we look for relevant natural laws that constrain solutions and reduce the instability of the problem. If the phonon spectrum is relatively smooth, and oscillations with extremely high frequencies can be ignored, then it is likely that the Hadamard instability can be cancelled or neglected.

### 2.3. Cancelling divergences with the parameter $s$ and calculating the Fourier transform

$C_V(T)$  is transformed into  $Q_0(x)$  using equation (4). By introducing the parameter  $s$  to cancel divergences [2], one can guarantee the existence of the Fourier transform in the inversion formula, independent of the Riemann hypothesis and Hadamard's proof, and simultaneously improve convergence.

In general, one can choose any  $s$  within the region  $0 = s_1 < s < s_2 \approx D$ . In this work, we use  $s = 1.5$  to improve convergence as well as avoid divergences. This can also reduce the data weights in the unmeasured region. The inversion formula is actually independent of the value of  $s$  as long as  $s$  is within the allowed range [2, 14]. However, because our calculation is numerical, the value of  $s$  weakly influences the final result. The selection of  $s$  then becomes important for general inversion problems. We find numerically very little sensitivity to  $s$  if it lies between 1.2 and 1.8, for a calculation with a few universal function terms. If the value is too large or small, numerical instabilities result.

At first glance, it may appear that fast Fourier transform (FFT) could be used for the Fourier transform in SPI, but FFT does not work as expected in this problem. The main reason is that for large enough  $k$ ,  $\tilde{F}_0(k) \equiv \tilde{Q}_0(k)[\Gamma(ik + s + 2)\zeta(ik + s + 1)]^{-1}$  can increase, due to insufficient accuracy of data, and one should cut off the calculation at a certain  $k$ . Also, in FFT one must choose a certain (finite) interval. In many cases, the cut-off interval  $\Delta k$  is not large enough for a concrete SPI problem. Finally, the spacing of sampling points is fixed in FFT. One cannot take many sampling points with very small spacing. Unfortunately, one does not know in advance how to cut  $k$ , so perhaps valuable information may be missed or errors could be introduced.

In order to work over a large scale of  $k$ , or in the infinite interval, one must improve the computing accuracy of  $\tilde{Q}_0(k)$  and its denominator. The main difficulty comes from the denominator: as  $k \rightarrow \infty$  the factor  $\Gamma(ik + s + 1)$ , does not go to infinity, as it would for a real argument, but it goes exponentially to zero:

$$\Gamma(z) = A(s)^{s+\frac{1}{2}} \exp\left\{-k \tan^{-1}\left(\frac{k}{s+1}\right)\right\} \sqrt{2\pi} \\ \times \exp\left\{ik \ln A(s) + i\left(s + \frac{1}{2}\right) \tan^{-1}\left(\frac{k}{s+1}\right) - (ik + s + 1)\right\} \left[1 + O\left(\frac{1}{z}\right)\right] \quad (9)$$

where  $A(s) = \sqrt{k^2 + (s+1)^2}$  and  $z = ik + s + 1 = A(s) \exp\{i \tan^{-1}(\frac{k}{s+1})\}$ . Necessary and sufficient conditions for the existence of the Fourier transform require that  $\tilde{F}_0(k)$  must tend to zero as  $k \rightarrow \pm\infty$ . In this case, using equations (9) and (3) we can find an improved unique existence theorem for our problem.

#### 2.4. An improved unique existence theorem

It is straightforward, from the necessary and sufficient conditions for the existence of the Fourier transform, that the necessary and sufficient asymptotic behaviour condition

$$|\tilde{Q}_0(k)| = o[|\zeta(ik + s + 1)\Gamma(ik + s + 2)|] = o\left[k^{s+\frac{3}{2}} \exp\left\{-k \tan^{-1}\left(\frac{k}{s+2}\right)\right\}\right], \quad (10)$$

ensures that equation (3) is a unique, exact solution to the specific heat equation (2).

Here the main improvement is that the condition is necessary and sufficient, but it is in  $k$  space.

#### 2.5. Calculating $\Gamma(z)$ and $\zeta(z)$

From the improved unique existence theorem, we see that the special functions  $\Gamma(z)$  and  $\zeta(z)$  should be calculated to high accuracy. The following expression is useful to get an accuracy of  $10^{-9}$  keeping only the first five terms. Denoting  $z = ik + s + n + 1$  and  $n = 9$ ,

$$\Gamma(ik + s + 1) = \frac{e^{-z} z^{z-\frac{1}{2}} \sqrt{2\pi}}{\prod_{j=1}^8 (ik + s + j)} \left\{ 1 + \frac{1}{12z} + \frac{1}{288z^2} - \frac{139}{51\,840z^3} - \frac{571}{2488\,320z^4} + o(z^{-5}) \right\}. \quad (11)$$

The main difficulty in calculating  $\Gamma(z)$  is due to complex arguments, for which  $\Gamma(z)$  is very different than for real arguments. Once one is aware of the pitfalls, the problem can be solved readily. Then the only difficulty is to maintain the numerical accuracy of the special functions.

To calculate  $\zeta(ik + s + 1)$ , instead of using the Dirichlet formula,

$$\zeta(z) = \sum_{n=1}^{\infty} \frac{1}{n^z},$$

we apply the Hardy formula (1929), which improves convergence:

$$\zeta(z) = \frac{1}{1-2^{1-z}} \sum_{n=1}^{\infty} \left[ \frac{1}{(2n-1)^z} - \frac{1}{(2n)^z} \right]. \quad (12)$$

For example, if  $s = 1.5$  and 1000 terms are taken into account, the relative accuracies of the Hardy formula and the Dirichlet formula are  $10^{-11.5}$  and  $10^{-3}$  respectively.

Using equations (11) and (12) to calculate the denominator of the integrand of equation (3) gives sufficient computational accuracy. The next problem is the calculation of  $\tilde{Q}_0(k)$ . This is the major difficulty in applying inversion to a concrete problem.

#### 2.6. Asymptotic behaviour control (ABC) and a suitable basis

Because the oscillating denominator goes to zero exponentially, the numerator of the inverse Fourier transform must go to zero more quickly than the denominator does. This is both a mathematical (for convergence) and a physical requirement. But we cannot expect the limited accuracy of experimental data to guarantee this asymptotic behaviour for large  $k$ . This is the reason that  $\tilde{F}_0(k)$  increases after a certain  $k$  in some practical calculations. The best way to overcome this is to reduce the weights of  $\tilde{F}_0(k)$  for large  $k$ . According to our theorem, one can only search for the solution within a function class in which  $C_V(T)$  satisfies the condition (10). One of the best ways is to expand the  $C_V(T)$  or  $\tilde{Q}_0(x)$  in a complete set of basis functions. This is also the best way simultaneously to improve the compactness of the sampling points of  $g(\omega)$ .

An ideal function set should satisfy the following conditions: it automatically complies with the required asymptotic behaviour given by equation (10). It is complete so it can cover all possibilities. It is helpful for the set to be orthogonal and normalized, because then it results in a unique expansion which simplifies finding the coefficients in numerical calculations.

We have found that the Hermite function set is one of the best for the present problem. The Hermite function set is complete and orthonormal in  $(-\infty, \infty)$ ; it is simple to use and results can be expressed analytically. The Hermite functions are related simply to the Hermite polynomials:

$$u_n(x) = \left( \frac{\alpha}{\sqrt{\pi} 2^n n!} \right)^{1/2} \exp\left(-\frac{1}{2}\alpha^2 x^2\right) H_n(\alpha x) \quad (n = 0, 1, \dots). \quad (13)$$

We can expand any  $Q_0(x)$  as

$$Q_0(x) = \sum_n c_n u_n(x), \quad (14)$$

and its Fourier transform can be found exactly and analytically, needing no additional numerical calculations to obtain

$$\tilde{u}_l(k) = (-i)^l \left( \frac{1}{2\pi\alpha} \frac{1}{\sqrt{\pi} 2^l l!} \right)^{1/2} \exp\left(-\frac{k^2}{2\alpha^2}\right) H_l\left(\frac{k}{\alpha}\right) \quad (15)$$

and

$$\tilde{Q}_0(k) = \sum_l c_l \tilde{u}_l(k). \quad (16)$$

It is important to note that expression (16) guarantees that  $\tilde{Q}_0(k)$  automatically satisfies the asymptotic behaviour stipulated by equation (10).

The expansion coefficients can be obtained using the orthonormality of the Hermite function set. So

$$c_l = \int_{-\infty}^{\infty} u_l(x) Q_0(x) dx. \quad (17)$$

We can obtain an explicit and useful expression for the functions in this set by using recurrence relations among the coefficients directly:

$$H_n(x) = \sum_{\mu=0,1}^n (-1)^{\frac{n-\mu}{2}} 2^{\frac{n+\mu}{2}} [1 \cdot 3 \cdot 5 \cdots (n-\mu-1)] C_n^{n-\mu} x^\mu, \quad (18)$$

where when  $n$  is even,  $\mu$  starts from zero, while if  $n$  is odd,  $\mu$  starts from unity, and  $C_n^{n-\mu}$  are the binomial coefficients.

### 3. Universal function set

As seen above, one can expand the  $Q_0(x)$  (obtained from the experimental specific heat  $C_V(T)$ ) as a series of Hermite functions  $u_n(x)$ . Using our exact solution formula (3), one can then obtain the phonon spectrum directly as

$$g(\omega) = \sum_l c_l G_l(\omega), \quad (19)$$

where  $\{G_l(\omega)\}$  is a (purely mathematical) UFS that is system independent:

$$G_l(\omega) = \frac{1}{\omega} \int_{-\infty}^{\infty} \left( \frac{\omega}{T_0} \right)^{ik+s} \frac{\tilde{u}_l(k) dk}{\Gamma(ik+s+2)\zeta(ik+s+1)}. \quad (20)$$



This UFS can be calculated in advance, even before we have  $C_V(T)$  data and the expansion coefficients  $c_l$ , which depend on the particular system. So we have calculated the UFS to high accuracy. We can fix  $s$  and  $T_0$  in advance. For example, we took  $s = 1.5$ ,  $T_0 = 50$  K. Therefore, for practical use, one need only measure  $C_V(T)$ , then obtain the expansion coefficients  $\{c_l\}$  by the integration (17). At that point, the phonon spectrum can be found by the summation (19). We refer to this approach using a UFS as the UFM.

One must be very careful in calculating the UFS, because the integrands in equation (20) oscillate rapidly. For large  $l$ , the integration is complicated and efficient integration methods are definitely needed. This UFS is not made up of elementary functions, but depends on numerical calculations. So for a given  $l$ , many sampling points must be taken into account, and the computations are time consuming.

For the integration from  $-\infty$  to  $\infty$ , one can divide the region, for example, into 14 segments:

$$(-\infty, -12], (-12, -10], \dots, (-2, 0], (0, 2], \dots, (10, 12], (12, \infty).$$

In the finite segments, Gauss–Legendre integration was used, while Gauss–Laguerre integration was applied to the integrals over  $(12, \infty)$  and  $(-\infty, -12]$ .

The Gauss–Legendre weighted integration formula is

$$\int_a^b f(y) dy \cong \frac{b-a}{2} \sum_{i=1}^n w_i f(y_i),$$

with

$$y_i = \left(\frac{b-a}{2}\right)x_i + \left(\frac{b+a}{2}\right),$$

where  $x_i$  is the  $i$ th zero of the Legendre polynomial  $P_n(x)$  and the Gaussian weight is  $w_i = \frac{2}{(1-x_i^2)}|P'_i(x_i)|^2$ . All of the values, such as  $x_i$  and  $w_i$ , can be found in tables of mathematical functions, e.g. [15].

The Gauss–Laguerre integration formula is

$$\int_0^\infty g(z) dz = \sum_{i=1}^n r_i e^{z_i} g(z_i),$$

where the points  $z_i$  and the weights  $r_i$  can also be found in tables of mathematical functions [15].

We have calculated the UFS  $\{G_l(\omega)\}$  with high accuracy. Examples of these functions are shown in figures 1 and 2.

#### 4. Results, discussion and concluding remarks

Applying the theory to actual data inevitably entails many difficulties. This work and our initial work represent the first attempt to apply the exact solution formula to a practical problem. We have overcome many of the mathematical difficulties, and we have been fortunate to find suitable experimental data. The improved unique existence theorem was proven and the UFS has been calculated in detail. Finally, the inversion results are shown in figure 3. This is the first successful inversion of real specific heat data to obtain the phonon spectrum. These results are discussed further below.

Incompleteness of the experimental data is one of the main difficulties for inverse problems. Because of this, many inverse problems cannot be solved in concrete instances. But this difficulty was overcome by using physical criteria for ABC in this problem. The instability of the solution due to an ill posed problem was overcome by finding a suitable basis set

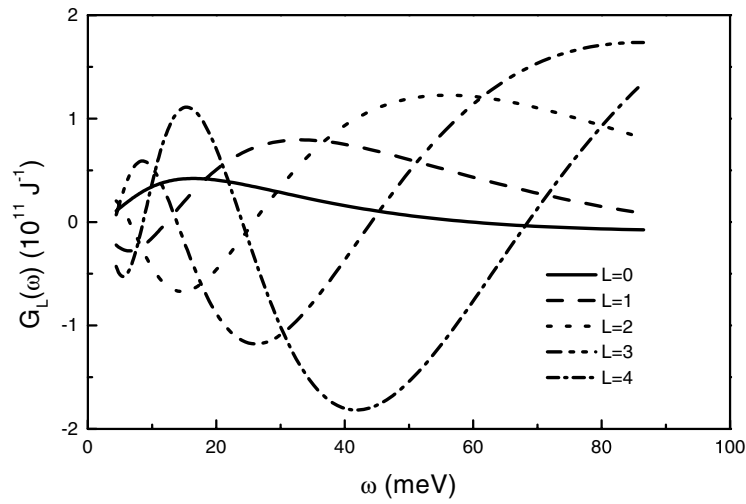


Figure 1. UFS, for  $L$  from 0 to 4.

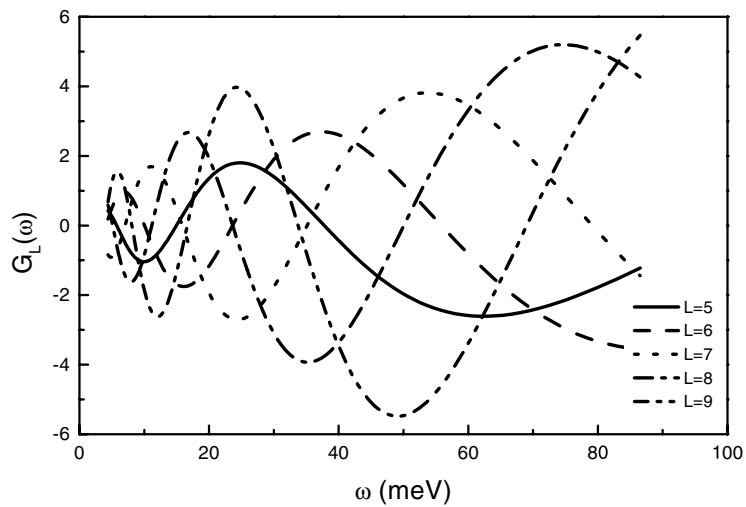
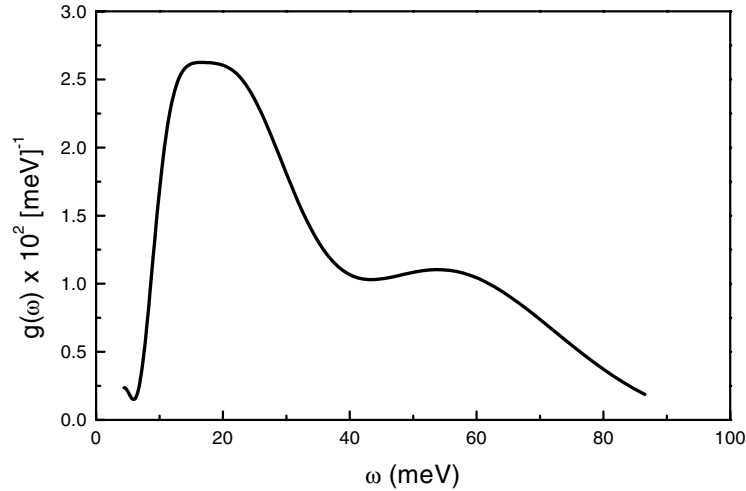


Figure 2. UFS, for  $L$  from 5 to 9.

consistent with the asymptotic behaviour constraints. We have limited the function class of possible solutions (not considering solutions with extremely high frequency oscillations), and thereby avoided Hadamard's instability. The improved unique existence theorem is a rigorous requirement for concrete problems, and it is one of the reasons that some methods cannot obtain correct results for practical problems. The basis set we selected was also chosen to satisfy the theorem, and the UFS  $\{G_l(\omega)\}$  was calculated with high accuracy. This function set is system independent and now makes possible practical calculations of SPI for other data sets.



**Figure 3.** Phonon spectrum (curve) calculated from experimental specific heat data by UFM carried to 30 terms.

#### 4.1. Concrete realization of the phonon spectrum

According to the UFM's fundamental formulae (19) and (20), the major work is in calculating the UFS and the coefficients  $c_l$ . The UFS can be calculated in advance. Then, in practice, one need only find the coefficients from experimental specific heat data by equation (17). In this work, experimental data for the specific heat of  $\text{YBCO}_{6.92}$  (equation (8)) were used to obtain the coefficients. Then the inversion results were obtained from equation (19) and are shown in figure 3. The parameters are  $s = 1.5$ ,  $\alpha = 1.0$  and  $T_0 = 50$  K, respectively. The first 30 members of the UFS were summed to obtain the results.

The results show the following.

- (1) The phonon spectrum of YBCO has an acoustic peak, in good agreement with that obtained by neutron inelastic scattering [11], including both the location (at about 20 meV) and the relative heights of the peaks;
- (2) It is well known that the phonon spectrum changes with oxygen concentration. For neutron inelastic scattering, the spectrum contains complicated structure. We only expect SPI to obtain the global features of the spectrum, given the limitations in the data and the approximations that had to be made. It is interesting that our results show a plateau at high frequencies in the region from 40 to 80 meV, where a second peak is observed in the neutron scattering experiments. This is in *qualitative* agreement with the experiments [11]. It is also interesting that there is a shoulder or hint of a small peak at about 50 meV. In fact, at high frequencies, the experiments also show a shoulder, but there are significant differences of detail. It is easy to understand that in this region the accuracy of the results is low because the integral kernel in equation (3),  $(\omega/T)^2 \exp(\omega/T) [\exp(\omega/T) - 1]^{-2}$ , decreases exponentially. To get information at high frequencies requires higher-accuracy experimental data. Nevertheless, both the acoustic peak height and the overall range of the inverted phonon spectrum are in good agreement with the neutron scattering result.
- (3) The ill-posedness of the problem is serious in inverse problems. But it has been reduced by ABC. Overall accuracy can be controlled by physical constraints, but this is still a delicate issue.

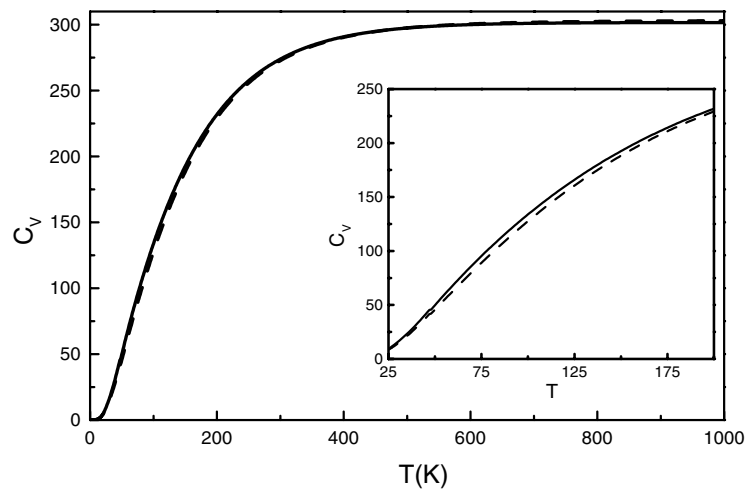


**Figure 4.** Effect on the experimental specific heat of an additional Gaussian peak at  $\omega = 42$  meV into the phonon spectrum.

#### 4.2. Effects of experimental errors

We explored the effect of introduced errors by adding a Gaussian peak of selected energy, of width 5 meV and normalized to 0.26 N (so it represents 8.8% of the spectral weight), to the phonon spectrum. This peak approximately mimics a corresponding peak in the experimental phonon spectrum. We then observed the effect of this extra peak on the specific heat.

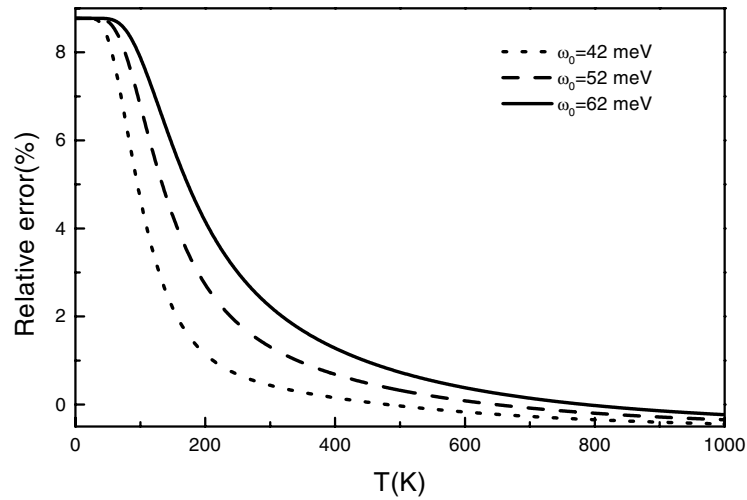
In figure 4, we show the effect on the specific heat of a Gaussian peak of energy 42 meV. Note that most of the effect of this extra peak lies in the temperature range 50–200 K, where the specific heat is depressed slightly. So relatively small errors in the experimental specific heat in this temperature range, especially if systematic, can hide (or introduce) a peak in the phonon spectrum.

Figure 5 shows the temperature dependence of the relative error in specific heat due to an additional Gaussian peak in the phonon spectrum at three different energies. The largest effect is at low temperature, but as the energy of the extra feature in the phonon spectrum increases we see a broadening of the temperature range over which the specific heat is sensitive. So, in order for SPI to obtain a peak like the extra test peak we used, the low-temperature specific heat would have to be found to greater relative accuracy at the lowest temperatures. This effect is emphasized further in figure 6, where we show absolute errors for the same effects.

After detailed investigations, we have found that phonon spectra are especially sensitive to changes of the specific heat in the temperature range 50–200 K. So it is important to improve the accuracy of the measured specific heat in this region.

#### 4.3. Comparison of experimental specific heat and that deduced from the neutron scattering phonon spectrum

The phonon spectrum from inelastic neutron scattering can be used in a direct calculation to obtain the specific heat, i.e. equation (2). This calculation is not sensitive to most of the difficulties that the inverse problem encounters. However, the specific heat which is calculated in this way does not agree well with the measured specific heat, as seen in figure 7.



**Figure 5.** Relative error in the specific heat due to an additional phonon spectrum peak at 42, 52 or 62 meV.

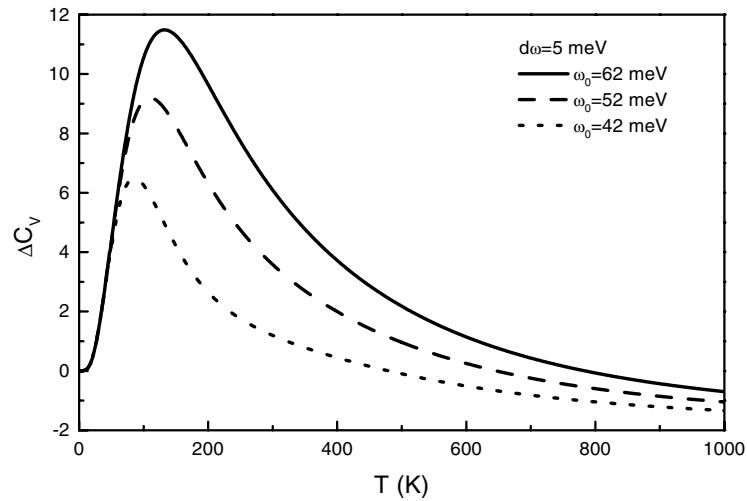


**Figure 6.** Absolute error in the specific heat due to an additional phonon spectrum peak at 42, 52 or 62 meV.

The measured phonon spectrum underestimates the specific heat for low temperatures and overestimates it for high temperatures. This effect is possibly related to the differences between our inverted phonon spectrum and that obtained from inelastic neutron scattering. We are continuing our exploration of these problems.

#### 4.4. This inversion method versus FFT

Before using UFM, we have applied FFT to this problem but could not obtain a satisfactory phonon spectrum. The main problems are computing precision and lack of ABC. The cut-off of  $k$  cannot be avoided. If one cuts off  $k$  at small values of  $\tilde{F}_0(k)$ , the results only have one phonon peak.

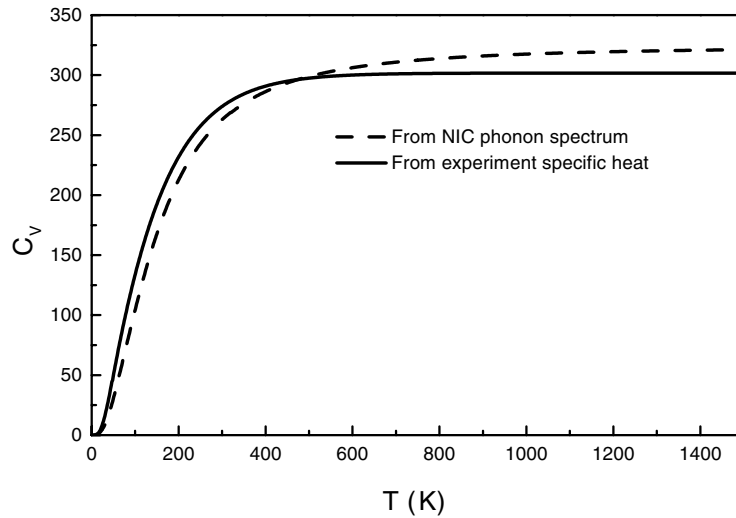


**Figure 7.** Comparison between experimental specific heat and the specific heat obtained from the neutron inelastic scattering phonon spectrum.

Another problem is that results cannot be obtained for arbitrary  $\omega$  because if  $\Delta k$  is given, the spacing of  $\omega$  in the phonon spectrum is thereby fixed. In fact, one can only obtain a very few points of the spectrum by FFT.

In our method all these problems are avoided. Because the asymptotic behaviour of the specific heat at high temperatures is controlled, the Fourier transform can be controlled. Divergences do not appear and the need for a cut-off is avoided. In our method the Fourier transform of the Hermitian function set is an analytic procedure and many unnecessary numerical calculations can be avoided.

#### 4.5. Comparison to Chen's Möbius inversion [3]

The exact solution formula in [1] is in closed form. It can obtain both the Einstein and Debye spectra exactly, including the important cut-off factor [16]

The modified Möbius inversion formula due to Chen [3] is a new series solution in physics. For the Debye spectrum, it can obtain the  $\omega^2$  term, but with no cut-off factor. The Möbius function for very large integers is unknown, because it depends on the prime factors of these integers, and we may not even be able to decide whether a particular large integer is prime, let alone be able to factor those which are not. So it may be difficult to get exact solutions from Chen's approach.

For practical applications, the Möbius inversion formula needs a large number of Laplace transforms and inverse Laplace transforms (back and forth). But our formula only needs a single Fourier transform (back and forth). So we believe our approach is more practical for applications.

With the aid of the UFS, one need only make an orthogonal expansion of  $Q_0(x)$ . Then the error can be controlled primarily by the quality of the input. The ill posed problem difficulties and problems from incompleteness of the data can be reduced by ABC and the consequent UFS.

In conclusion, the UFM has been shown to be useful and practical for real systems.

## Acknowledgments

One of the authors (XXD) would like to acknowledge Professors C N Yang, Yu Lu and Ma Yongli, and the research group in theoretical physics at Brigham Young University (BYU) for significant discussions. He would also like to thank the Department of Physics and Astronomy at BYU for their hospitality. This work is in projects 10174016, 19834010 and 19975009 and supported by the National Science Foundation of China.

## References

- [1] Dai XianXi, Xu XinWen and Dai JiQiong 1989 *Proc. Int. Conf. on High  $T_c$  Superconductivity (Beijing, China, 1989)* p 521
- [2] Dai XianXi, Xu XinWen and Dai JiQiong 1990 *Phys. Lett. A* **147** 445
- [3] Chen N X 1990 *Phys. Rev. Lett.* **64** 1193
- [4] Maddox J 1990 *Nature* **344** 377
- [5] Hadamard J 1896 *Bull. Soc. Math. France* **24** 199
- [6] Montroll E W 1942 *J. Chem. Phys.* **10** 218
- [7] Lifshitz I M 1955 *Zh. Eksp. Teor. Fiz.* **26** 551
- [8] Chambers R G 1961 *Proc. Phys. Soc.* **78** 941
- [9] Bessergenev V G, Kovalevskaya Yu A, Naumov V N and Frolova G I 1995 *Physica C* **245** 36
- [10] Ginsberg D M 1994 *Physical Properties of High Temperature Superconductors* vols 1–4 (Singapore: World Scientific)
- [11] Renker B, Gompf F, Gering E, Ewert D, Rietschel H and Dianoux A 1988 *Z. Phys. B* **73** 309
- [12] Landau L D and Lifshitz E M 1980 *Statistical Physics* (Oxford: Pergamon)
- [13] Dai XianXi, Dai JiXin and Dai JiQiong 1997 *Phys. Rev. A* **55** 2617
- [14] Wen Tao, Ming DengMing, Dai XianXi, Dai JiXin and Evenson W E 2001 *Phys. Rev. E* **63** 045601(R)1-4
- [15] Abramowitz M and Stegun I A 1972 *Handbook of Mathematical Functions* (New York: Dover)
- [16] Ming DengMing, Wen Tao, Dai JiXin, Dai Xianxi and Evenson W E 2000 *Phys. Rev. E* **62** R3019–22